MD Simulations of Homomorphous PNA, DNA, and RNA Single Strands: Characterization and Comparison of Conformations and Dynamics

Srikanta Sen[†] and Lennart Nilsson*

Contribution from the Department of Bioscience at NOVUM, Center for Structural Biochemistry, Karolinska Institutet, S-14157, Huddinge, Sweden

Received September 5, 2000

Abstract: MD simulations of homomorphous single-stranded PNA, DNA, and RNA with the same base sequence have been performed in aqueous solvent. For each strand two separate simulations were performed starting from a (i) helical conformation and (ii) random coiled state. Comparisons of the simulations with the single-stranded helices (case i) show that the differences in the covalent nature of the backbones cause significant differences in the structural and dynamical properties of the strands. It is found that the PNA strand maintains its nice base-stacked initial helical structure throughout the 1.5-ns MD simulation at 300 K, while DNA/RNA show relatively larger fluctuations in the structures with a few local unstacking events during -ns MD simulation each. It seems that the weak physical coupling between the bases and the backbone in PNA causes a loss of correlation between the dynamics of the bases and the backbone compared to the DNA/RNA and helps maintain the base-stacked helical conformation. The global flexibility of a single-stranded PNA helix was also found to be lowest, while RNA appears to be the most flexible single-stranded helix. The sugar pucker of several nucleotides in single-stranded DNA and RNA was found to adopt both C2'-endo and C3'-endo conformations for significant times. This effect is more pronounced for single strands in completely coiled states. The simulations with single-stranded coils as the initial structure also indicate that a PNA can adopt a more compact globular structure, while DNA/RNA of the same size adopts a more extended coil structure. This allows even a short PNA in the coiled state to form a significantly stable nonsequentially base-stacked globular structure in solution. Due to the hydrophobic nature of the PNA backbone, it interacts with surrounding water rather weakly compared to DNA/RNA.

Introduction

Recently, different DNA analogues have been developed mainly by modifying the backbone of the DNA strand.[1−4] Peptide nucleic acid (PNA) is one such DNA analogue. A PNA molecule is essentially a DNA strand where the usual sugar−phosphate backbone has been replaced by a structurally homomorphous pseudopeptide chain consisting of *N*-(2-amino-ethyl)-glycine units (Figure 1).[5−8] There are two major differences between PNA and DNA/RNA: (i) PNA is electrically neutral, while DNA/RNA are negatively charged, and (ii) unlike DNA/RNA where the backbone contains a sugar ring to which the base is attached, in PNA the base is connected to the backbone through a short chain containing only single bonds. The RNA

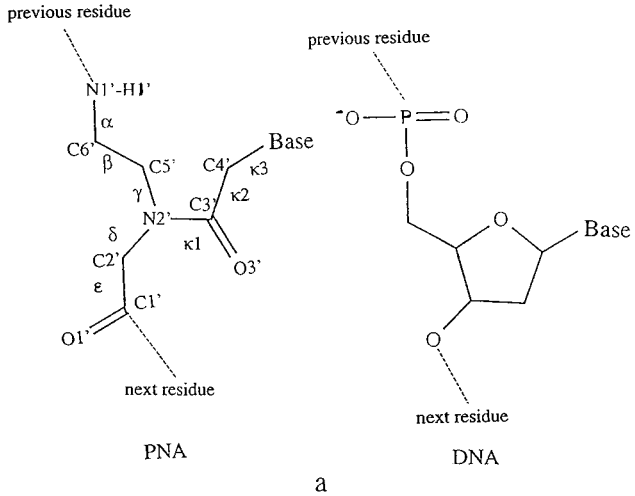

Figure 1. (a) Schematic diagrams show the difference of a PNA and a DNA monomeric unit. (b) Base sequence used for PNA, DNA, and RNA.

* To whom correspondence should be addressed.
[†] Present address: Theoretical Biology Group, Biophysics Division, Indian Institute of Chemical Biology, 4, Raja S. C. Mullick Road, Calcutta-700032, India.

(1) Nielsen, P. E.; Egholm, M.; Berg, R. H.; Buchardt, O. *Science* **1991**, 254, 1497−1500.
(2) Kuwahara, M.; Arimitsu, M.; Sisido, M. *J. Am. Chem. Soc.* **1999,** 121, 256−257.
(3) Koshkin, A. A.; Nielsen P.; Melgaard, M.; Rajwarshi, V. K.; Singh, S. K.; Wengel, J. *J. Am. Chem. Soc.* **1998**, 120, 13252−13253.
(4) Dempsy, R. O.; Browne, K. A.; Bruce, T. C. *J. Am. Chem. Soc.* **1995**, *117*, 6140.
(5) Egholm, M.; Buchardt, O.; Nielsen, P. E.; Berg, R. H. *J. Am. Chem. Soc.* **1992**, *114*, 1895−1897.
(6) Egholm, M.; Buchardt, O.; Christensen, L.; Behrens, C.; Freier, S. M.; Driver, D. A.; Berg, R. H.; Kim, S. K.; Nordén. B.; Nielsen, P. E. *Nature* **1993**, 365, 566−568.
(7) Nielsen, P. E. *Annu. Rev. Biophys. Biomol. Struct.* **1995**, 24, 167−183.
(8) Eriksson, M. E.; Nielsen, P. E. *Q. Rev. Biophys.* **1996**, 29, 369−394.

10.1021/ja0032632 CCC: $20.00
Published on Web 07/10/2001

backbone is also slightly different from that of DNA due to the presence of the ribose sugar. Thus, PNA, DNA, and RNA constitute a novel set of molecules for investigating how much of the differences in structural and dynamical properties of these homomorphous molecules are due only to changes in the backbones. Furthermore, detail investigations on the structural and dynamical properties of single-stranded nucleic acids are also part of the recent research interests.

PNA molecules are interesting also from another point of view. It is now experimentally well established that PNA can bind to DNA/RNA with complementary base sequences to form a double helices with higher affinity compared to that of DNA−DNA or RNA−RNA binding in duplexes. This makes PNA a potential candidate as a gene targeting and antisense agent in gene therapy.[5−8] Recent studies have shown that PNA also possess some other properties essential for a genetic drug.[9−12] To function as a gene targeting or antisense agent, PNA must be used as a single-stranded molecule. Thus, in the case of PNA, it is additionally important to characterize the details of the structural and dynamical properties of a single strand. Such knowledge may also be useful in developing new tailor-made nucleic acid analogues with more desired properties.

In a recent work,[13] we have investigated the structural and dynamical properties of duplexes involving PNA molecules by using molecular modeling and molecular dynamics simulation techniques, where we obtained results in excellent agreement with available experimental data. The success of that work has encouraged us to extend our work with PNA, DNA, and RNA further. In the present work we have employed molecular modeling and molecular dynamics simulation techniques for studying and comparing the structural, interactional, and dynamical properties of single-stranded oligomers (PNA, DNA, and RNA) which have the same base sequence but chemically different backbones.

We have carried out systematic studies of independent unrestrained MD simulations of single strands of (i) PNA, (ii) DNA, and (iii) RNA in aqueous solution under periodic boundary conditions and have compared their properties. For each single strand, we have prepared two independent setups. In one case we started with the respective single strand in a helical conformation with all of the bases properly stacked sequentially on the top of each other. In the other setup, the initial structure used was a random coil conformation generated by high-temperature dynamics simulation of the strand. We have performed MD simulations in the same way for each single strand such that the results of each single strand can be directly compared with those of others. The results show that the structural and dynamical properties of the single-stranded molecules can be quite different, depending on the nature of the backbones even though they are homomorphous to each other. We discussed the possible physical origins of the observed differences in terms of the covalent nature of the backbones. However, as not much quantitative experimental data are available for such single-stranded molecules, it has only been possible to compare our results with the experimental qualitative information wherever available. The results of the present study develop a detailed picture of the differences in the structural and dynamical properties of single strands having backbones of different nature and also provide us with useful insights in understanding the physical basis of these observed differences in properties.

Methods

(i) Topology and Parameters. For the single-stranded DNA and RNA the standard CHARMM nucleic acid residue topology and parameters[14] were used. However, as PNA molecules are not common biomolecules, the topology and parameters for PNA residues are not directly available in the standard CHARMM[15]nucleic acid residue topology and parameters.[14] In our previous work[13] we have prepared these relevant parts for PNA for use in CHARMM. We have assigned the atom types of the atoms involved in PNA residues following CHARMM[15] atom-type definitions. This makes most of the bond, angle, dihedral, and all of the nonbonded parameters directly available from the combined CHARMM all-hydrogen parameter set for nucleic acids and proteins.[14] Those, which are not available, were obtained by comparison with similar groups in the CHARMM parameter set.[14] In the present work we have used the same topology and parameter sets for PNA strands. The partial atomic charges for the atoms in PNA residues were estimated by the ESP (ElectroStatic Potential) method in the MOPAC 6.0 package[16] by fitting the partial atomic charges to reproduce the electrostatic potentials at 1448 space points around the molecule. The details are available in our previous work.[13] A representative of the topology file for PNA units is available as Supporting Information.

(ii) Preparation of Starting Models. The coordinates of the atoms in the single-stranded 10-mer DNA with the base sequence 5′-AGTGATCTAC-3′ in the B-helix form were generated with the program INSIGHT-II (Molecular Simulations Inc, San Diego), and the coordinates of the H-atoms were generated by the HBUILD[17] facility of CHARMM. Similarly, the coordinates of the atoms of the single-stranded 10-mer RNA of the same base sequence were generated in the A-helix form with INSIGHT-II. In each case the energy of the strand was minimized in a vacuum for 200 steepest descent steps to remove any local distortion or bad contacts.

For the single-stranded PNA we first generated the atomic coordinates of the single-stranded DNA in B-form. As a PNA backbone is superimposable on the corresponding DNA backbone, we then converted the single-stranded DNA into a single-stranded PNA simply by replacing the non-H atoms of the backbone of the respective DNA strand by the PNA backbone atoms following the one-to-one mapping scheme (DNA) O5′-C5′-C4′-C3′-C2′-C1′-O3′-+P-+O1P → N1′-C6′-C5′-N2′-C3′-C4′-C2′-C1′-O1′ (PNA). (DNA) C5′-C4′-C3′-C2′-C1′-O3′-+P-+O1P-+O5′ → C6′-C5′-N2′-C3′-C4′-C2′-C1′-O1′-N1′ (PNA) as described in our earlier work.[13] The coordinates of the H-atoms were generated by the HBUILD[16] facility in CHARMM. The resulting coordinates of the duplex were then energy-minimized in a vacuum for 300 steepest descent steps keeping the bases fixed in positions allowing only the newly generated backbone to relax. Then the restraints were removed, and further energy minimization for 200 steepest decent steps were performed. The PNA single strand was then used for subsequent MD simulation in a water box.

(iii) Setup of Solvated Systems. In the cases of single-stranded DNA or RNA, one Na^+ counterion per phosphate group was included for electrical charge neutralization of the system.[18] Each Na^+ ion was placed at a distance 3.5 Å from the phosphorus atom of the respective phosphate group, on a line bisecting the line joining the two oxygen atoms of the phosphate group. For PNA molecules no counterions were needed. The molecular system was then inserted in a rectangular water box of size 31.5 Å × 31.5 Å × 41.5 Å, containing 1288 preequilibrated

(9) Hamilton, S. E.; Simons, C. G.; Kathiria, I. S.; Corey, D. R. *Chem. Biol.* **1999,** *6*, 343−351.
(10) Nielsen, P. E. *Curr. Opin. Struct. Biol*. **1999**, 9, 353−357.
(11) Good, L.; Nielsen P. E. *Nature Biotechnol.* **1998**, 16, 355−358.
(12) Taylor, B. M.; McCormic, D. J.; Hoshall, C. V., Douglas C. L.; Jansen, K.; Lacy, B. W.; Cusack, B.; Rechelso, E. *FEBS Lett.* **1998**, 421, 280−284.
(13) Sen, S.; Nilsson, L. *J. Am. Chem. Soc.* **1998**, *121*, 619−631
(14) Brooks, B. R.; Bruccoleri, R. E.; Olafson, B. D.; States, D. J.; Swaminathan, S.; Karplus. M. *J. Comput. Chem.* **1983**, *4*, 187−217.
(15) MacKerell, A. D., Jr.; Wiorkiewicz-Kuczera, J.; Karplus, M. *J. Am. Chem. Soc.* **1995**, *117*, 11946−11975.
(16) Brunger, A.; Karplus, M. *Proteins: Struct., Funct., Genet.* **1988**, 4, 148−156.
(17) Coolidge, M. B.; Stewart, J. J. P. *MOPAC, 6.0;* ESCOM Science Publishers: Leiden, the Netherlands, 1990.
(18) Jayaram, B.; Beveridge, D. L. *Annu. Rev. Biophys. Biomol. Struct.* **1996,** 25, 367−394

TIP3P water molecules.[19] Water molecules that were closer than 2.8 Å from any atom of the solute molecule or counterion were deleted. This solvated system was energy-minimized for 500 steepest descent steps, keeping the solute fixed in position to allow only the counterions and water molecules to reorient themselves favorably around the solute. Subsequently, the constraint on the solute was removed, and energy minimization for another 500 Powell steps was done. The resulting systems were then used to perform the subsequent MD simulations.

For generating the single strands in unstacked nonhelical conformations in each case we performed MD simulations with the respective single strand in an initial base-stacked helical structure at a high temperature (1000 K) and selected a frame from the later part of the 100-ps trajectory. We minimized the energy of the frame and used it as the starting point for MD simulations at 298 K.

(iv) Dynamics Simulation Methodology. All MD simulations were done by employing the program package CHARMM, version 25, with its standard empirical potential energy function.[15] In the simulations, Newton's equation of motion for each atom, was integrated using the leapfrog-Verlet algorithm[20,21] with a time step of 2.0 fs. The SHAKE algorithm[22,23] was applied to constrain the bond lengths involving hydrogen atoms to their equilibrium positions. Periodic boundary conditions using minimum image conventions were applied in calculating the nonbonded interactions. The nonbonded pair list was updated every 10 steps using a 13 Å cutoff, and the nonbonded interaction energies and forces were smoothly shifted to zero at 12.0 Å. For electrostatic calculations a relative dielectric constant 1.0 was used.

It may be pointed out here that even though the present trend of handling the electrostatic interaction is to use PME or Ewald methods, we have used the force-shifted cutoff methods, which have been shown[24] to yield results very similar to those obtained when PME is used for DNA simulations. In a recent work[25] results on the properties of duplexes involving DNA, RNA, and PNA have been reported where the authors have used AMBER force field and the PME method in handling the electrostatics; these results are in very good agreement with the results in our previous work[13] where also we used force-shifted cutoff methods for nonbonded interactions. This shows that careful use of force-shifted cutoff methods can produce reliable data consistent with data obtained by using PME/Ewald methods for computing electrostatics. In a recent review[26] Cheatham and Kollman also mention that force-shifted cutoff methods (in the range 12−14 Å) can produce stable and reliable dynamics trajectories for nucleic acids.

In each simulation, the water box including the solvated solute was heated to 298 K during the first 2 ps and then equilibrated for 2 ps by assigning velocities to the atoms from a Gaussian distribution at 298 K. The simulation was continued with checking the temperature every 100 steps, and the temperature was adjusted by scaling velocities only if the average temperature of the system was outside the window 298 ± 10 K. Thus, the average temperature was maintained around 298 K. The size of the box was kept fixed during the simulation, making it effectively under a constant NVT condition. The trajectory was saved every 200 steps for analysis. MD simulation with single-stranded PNA was continued for 1.5 ns. Each of the systems with single-stranded DNA and RNA was simulated for about 1 ns. For single strands in coil conformation MD simulation was performed for 300 ps for each strand. Structural and dynamical analyses were then done over the appropriate parts of the respective trajectories in each case.

Hydrogen Bonds and Water Bridges. A 2.5 Å cutoff for hydrogen-acceptor distance and a 135° cutoff for the donor−hydrogen−acceptor angle was used in defining hydrogen bonds. A water bridge between two hydrogen-bonding atoms consists of one water molecule that simultaneously hydrogen bonds to the two other atoms. Hydrogen bonds and water bridges were analyzed in the trajectories with 4 ps time resolution.

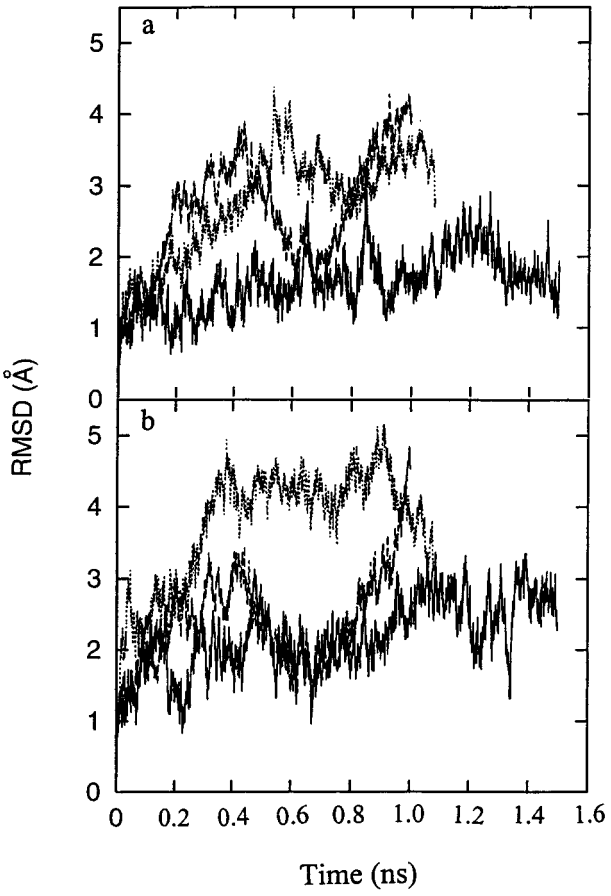

Figure 2. Time evolution of the RMSD of (a) the backbone and (b) the bases of the single-stranded PNA (solid line), DNA (dashed line), and RNA (dotted line).

Results and Discussion

(A) Structural Features. It is clearly seen from the root-mean-squared deviations (rmsd) in Figure 2a,b that the single-stranded PNA retained a defined (stable and ordered) structure close to its starting structure, while for both the DNA and the RNA the RMSD changed considerably with time, indicating that in these two cases the structures were deviating significantly from the respective starting structure and thus spanned over a wider range of conformational space during dynamics simulations. Figure 3a−c presents stereoviews of several snapshots of each of the three different kinds of single strands at different stages of the respective trajectories. Here it is also demonstrated that the PNA strand maintained its base-stacked ordered structure throughout its 1.5 ns long dynamics simulation trajectory, while for both DNA and RNA there were local disorders due to breakage of base stacking in a few places although a significant amount of base-stacked structure is maintained throughout their 1 ns long trajectories. There is experimental evidence indicating that single-stranded DNA or RNA does not adopt a completely extended conformation and does not possess significant amount of order in aqueous solvent.[27,28] It has further been shown from the NOE cross-

(19) Jorgensen, W. L.; Chandrasekhar, J.; Madura, J. D.; Impey, R. W.; Klein, M. *J. Chem. Phys.* **1983**, 79, 926−935.
(20) Hockney, R. W. *Methods Phys.* **1970**, *9*, 136−211.
(21) Potter, D. *Computational Physics*; Wiley: New York, 1972; Chapter 5.
(22) van Gunsteren, W. F.; Berendsen, H. J. C. *Mol. Phys.* **1977**, 34, 1311−1327.
(23) Ryckaert, J. P.; Ciccotti, G.; Berendsen, H. J. C. *J. Comput. Phys.* **1977**, 23, 327−341.
(24) Norberg, J.; Nilsson, L. *Biophys. J.* **2000**, 97, 1537−1553.
(25) Soliva, R.; Sherer, E.; Luque, F. J.; Laughton, G. C. A.; Orozco, M. *J. Am. Chem. Soc.* **2000**, 122, 5997−6008.
(26) Cheatham, T. E.; Kollman, P. A. *Annu. Rev. Phys. Chem.* **2000**, 51, 435−471.
(27) Tomac, S.; Sarkar, M.; Ratilinen, T.; Wittung, P.; Nielsen, P. E.; Nordén, B.; Gräslund, A. *J. Am. Chem. Soc.* **1996**, *118*, 5544−5552.

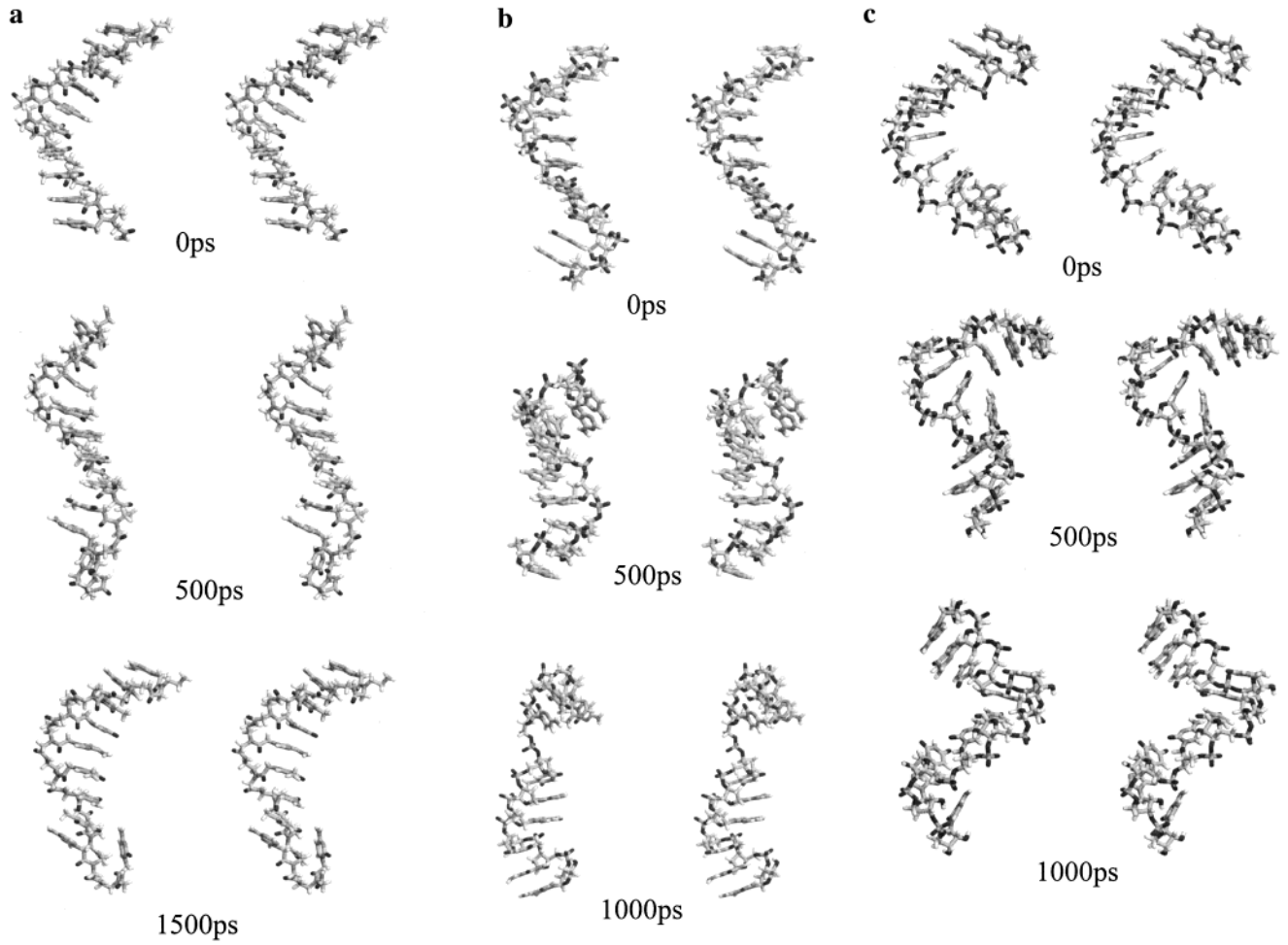

Figure 3. Snapshots of the different frames from the respective dynamic trajectory of the single-stranded (a) PNA, (b) DNA, and (c) RNA.

peaks patterns obtained in an NMR experiment with a single-stranded PNA octamer that it had a pre-organized single conformation.[29] Our findings on the single-stranded PNA, DNA, and RNA are thus in complete agreement with these results and provide further details of the structural and dynamical features of these molecules. It may also be mentioned here that the maintenance of the base-stacked helix-like structure of the single-stranded PNA is in accord with the currently emerging view that the helix structure of nucleic acids is mainly driven and stabilized by the base-stacking interactions.[30,31] It may be pointed out here that the large difference in the covalent nature of the connection of the bases to the backbone in PNA and DNA/RNA makes the physical coupling of the base to the backbone much weaker in PNA than in DNA/RNA as explained below. Here it is demonstrated that the weak coupling between the base and the backbone further helps maintaining base-stacked helical structure of single strands, allowing larger structural rearrangements in the backbone including the base-linker region.

It is further noticeable that in contrast to the case of a double helix, in the single strands the rmsd values are larger and more fluctuating with time during dynamics compared to those of the respective backbones.[13] The reason is simply the fact that in a single strand, in the absence of the complementary strand, the bases are not buried on the inside of the structure and thus are subjected to more dynamical freedom.

(B) Correlated Dynamics. To compare the correlated nature of the dynamics of the bases and the backbone in the three different kinds of single strands in helical conformations, we have considered the corresponding rmsd time series over the intermediate period (~100 ps) where each of them maintained a base-stacked ordered structure, and there is not much drift of the average rmsd value. The linear correlation coefficient (C_{xy}) between two similar data series can be calculated by the relation

$$C_{xy} = \langle (x^i - x^i_{\text{ave}})(y^i - y^i_{\text{ave}}) \rangle / \{ \langle (x^i - x^i_{\text{ave}})^2 \rangle \langle (y^i - y^i_{\text{ave}})^2 \rangle \}^{1/2}$$

where x^i and y^i are the ith elements in the two data series respectively.[32] It is found that the linear correlation coefficient is very high (0.92 for the DNA and 0.87 for the RNA) for nucleic acids, while it is considerably lower (0.38) for PNA. This difference in the behavior between nucleic acids and PNA can be rationalized as follows. The covalent coupling between the backbone and the bases is quite strong, being mediated by a sugar ring in the case of nucleic acids, while the coupling is much weaker in PNA as in this case the base is linked to the backbone by a simple single-bonded chain. It seems that the strong coupling between the base and the backbone in the cases

(28) Vasnaver, G.; Breslauer, K. J. *Proc. Natl. Acad. Sci. U.S.A.* **1991**, 88, 3569−3573.
(29) Chen, S. M.; Mohon, V.; Kiely, J. S.; Griffith, M. C.; Griffey, R. H. *Tetrahedron Letters* **1994,** 35, 5105−5108.
(30) Matray, T. J.; Kool, E. T., *J. Am. Chem. Soc.* **1998**, *121*, 6191−6192
(31) Guckian, K. M.; Schweitzer, B. A.; Ren, R. X. F.; Sheils, C. J.; Puris, P. L.; Tahmassebi, D. C.; Kool, E. T. *J. Am. Chem. Soc.* **1996**, *118*, 8182−8183.
(32) Press: W. H.; Teukolski, S. A.; Vetterling, W. T.; Flannery, B. P. *Numerical Recipes in Fortran*, 2nd ed.; Cambridge University Press, New York, 1992; pp 630.

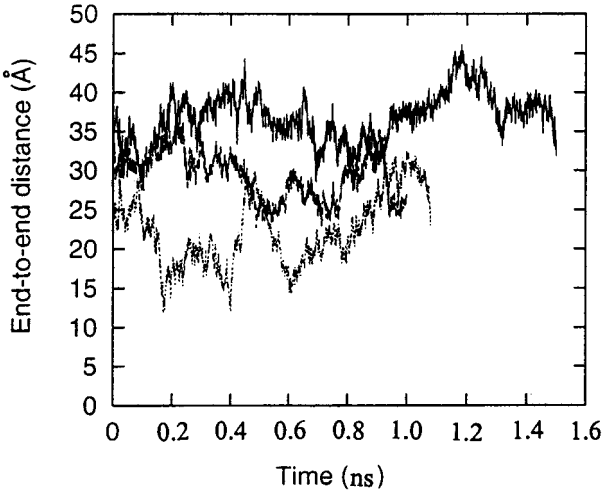

Figure 4. Comparison of the time evolution of the end-to-end distance of PNA (solid line) DNA (dashed line) and RNA (dotted line) backbones during dynamics simulation.

Table 1. Comparison of the Average, Fluctuation and the Nomalized Fluctuation of the End-to-End Distance of the Different Single Strand from the Dynamics Simulation in Water

	average (Å)	fluctuation(Å)	norm. fluc.
PNA	36.79	3.18	0.086
DNA	29.33	3.01	0.103
RNA	22.35	4.51	0.201

of DNA and RNA causes a few breaks of local base stacking during dynamics, while in the case of PNA the weaker base−backbone coupling allows the PNA single strand to maintain its base-stacked structure even in the presence of significant conformational changes in the backbone.

(C) Local and Global Flexibility. Figure 4 compares the time evolution of the end-to-end distance of each of the three different types of strands. The distance between the end backbone atoms (non-hydrogen) of each single strand was considered as the end-to-end distance in each case. It is indicated that during the dynamics simulations the end-to-end distance is more stable for the PNA strand than for the DNA or RNA where considerable fluctuations were observed. Table 1 summarizes the comparison. As the average end-to-end distance is different for different types of single strands, we have normalized the calculated fluctuations in each case by the corresponding average end-to-end distance so that we can directly compare the normalized fluctuations. From Table 1 it is found that the normalized fluctuation is largest for the RNA and lowest for the PNA. The difference in the fluctuation behavior may be due to the fact that the single-stranded PNA maintains a base-stacked ordered structure, while the DNA and the RNA unstack at several places of the single strand.

Figure 5a shows the distribution of the distances between two phosphorus atoms in the DNA/RNA strand or equivalently that between two N2′ atoms in the PNA strand. The PNA strand exhibits the most distinct pattern, indicating a well-defined ordered structure during the dynamics, and RNA shows the most broadened structure with overlapping peaks, particularly at longer separations. Figure 5b represents the same plots for each of the strands in their initial structure which is considered as a control to see if the structure (A-helix or B-helix) of the strand has any intrinsic overlapping feature in the plot. Broadening of the width of a peak in the plot compared to the control plot indicates an enhanced flexibility. If the broadening occurs for short separations it indicates an enhancement of the local

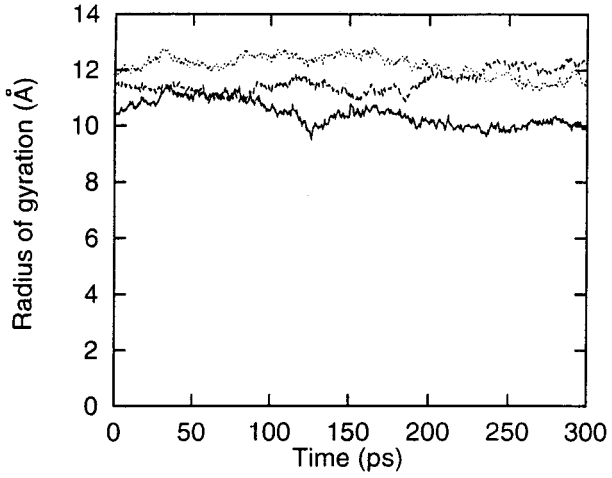

Figure 5. (a) Plot of the distribution of the P−P (phosphorus−phosphorus) for DNA (dashed) and RNA (dotted) and equivalently the N2'−N2' distance for PNA (solid) obtained from the dynamic trajectories of the respective single-stranded helices. (b) The same distribution in the initial structure (a single frame) demonstrating the distribution pattern that is intrinsic to the single-stranded PNA (solid), DNA (dashed) and RNA (dotted) helices to be used as a control.

flexibility, while widening of peaks at longer distance implies enhanced global flexibility. Comparison clearly indicates that the widths of the first peak for all three of the different single strands in Figure 5, a and b, are very similar, which implies that the local flexibilities of the different strands are very similar to each other. On the other hand, it is found that the widths of the peaks at longer separation are considerably broadened for the DNA and the RNA single strands compared to the PNA single strand, indicating that the global flexibility of PNA is less compared to that of DNA and RNA when they are in single-stranded helical structure. Another aspect that should be pointed out is that in Figure 5a the first peak is found at a very similar position for all three strands, while for PNA the successive peaks appear at slightly longer separation compared to those for the DNA/RNA. This occurs due to the large difference in the covalent nature of the backbones of PNA and DNA/RNA even though they are homomorphous to each other. Thus, it may happen that a long PNA strand will not be able to form a perfect double helix with a complementary DNA as the lengths of the DNA strand and the PNA strand will not match with each other. However, for short PNA fragments (say 15mer) it should not create any major problem as is found in reality.[5,8] To our knowledge, no data is available to date on the differences in the flexibility of the different single strands. However, interesting differences in the structural properties of single-stranded DNA and RNA have been observed in recent experiments using FTIR and other spectroscopic techniques.[33]

(D) Features of the Coiled states. The radius of gyration of a chain molecule is a useful measure to characterize the shape of a molecule of a given size and thus can be used to compare the globular or elongated nature of the coil-like chains in the present study. Figure 6 shows the time evolution of the radius of gyrations of the different types of single strands in coiled states. It is found that both DNA and RNA retain considerably extended conformations, while the PNA single strand adopts a more compact coiled configuration. This difference is completely in agreement with the fact that the intramolecular phosphate−phosphate electrostatic repulsion for both DNA and RNA forces them to maintain an elongated conformation, while

(33) Lindqvist, M.; Sarkar, M.; Winqvist, A.; Rozner, E.; Strömberg, R.; Gräslund, A. *Biochemistry* **2000**, 39, 1693−1701.

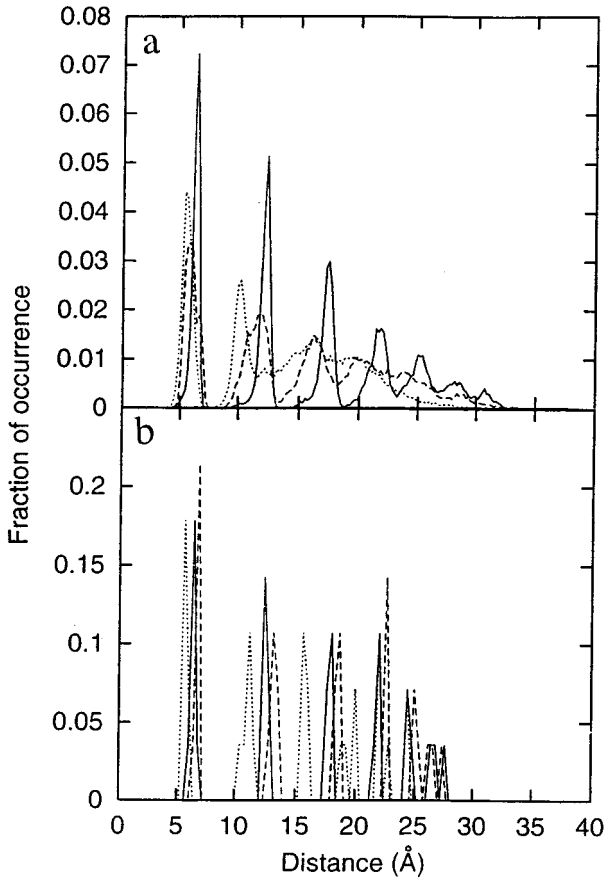

Figure 6. Comparison of the time evolution of the radius of gyration of the single-stranded PNA (solid) DNA (dashed) and RNA (dotted) molecules in the coiled conformations.

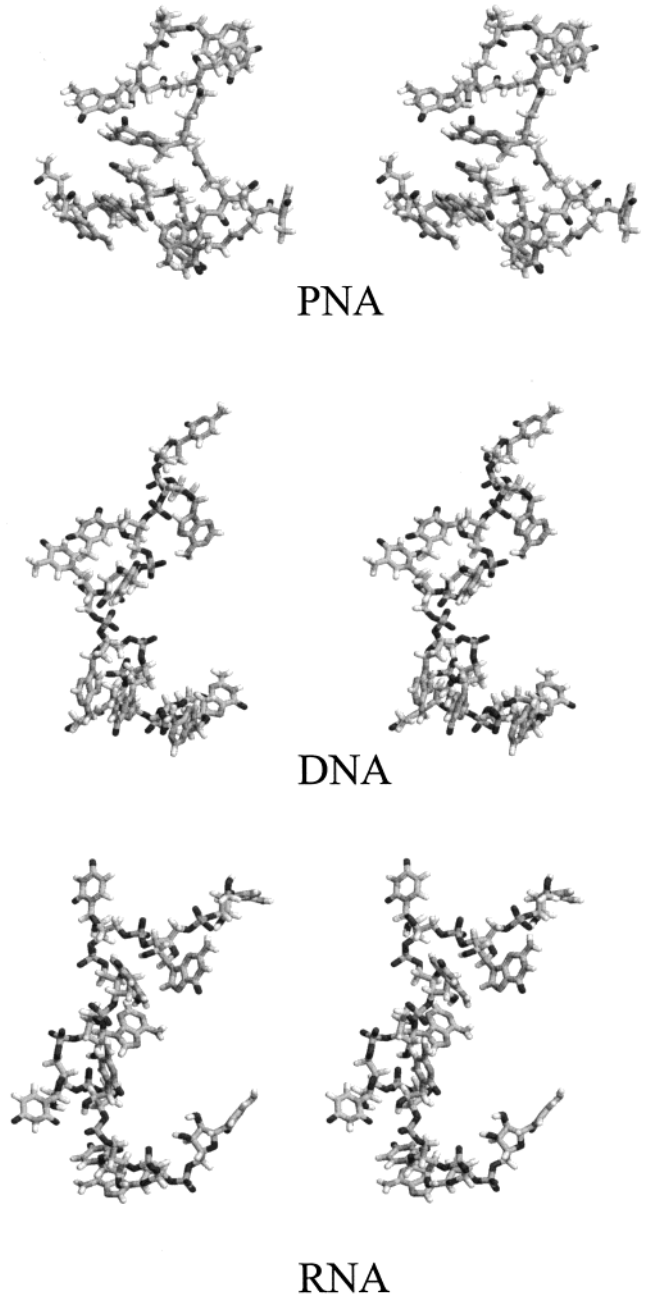

Figure 7. Stereoviews of the structures of the snaps of the coiled single strands at the 300th ps frame from the dynamic trajectories.

the absence of such a repulsion allows the PNA to adopt a more compact globular coiled configuration. Figure 7 shows the snapshots of the three different coiled single strands at the 300th ps frame which also clearly demonstrate the relatively elongated conformation of the DNA/RNA strands compared to the more globular PNA single-stranded coil. This also gives rise to a significant possibility in the case of PNA that, once the fully base-stacked helical structure is lost, it may fold back onto itself, forming other structures by making nonsequential base-stacking. From our MD simulation of PNA in the coiled state, without any initially stacked bases, we find that a considerable amount of random, that is, nonlocal in the linear base sequence, base stacking develops during the simulation. Thus, the base-stacked structure at room temperature is highly favored by a single-stranded PNA molecule but no intra-strand base pairing was found. Even for a short PNA such nonsequential base stacking may result in a sufficiently stable local minimum that it becomes difficult to revert back to helical conformation from a random coil conformation. In this case, the presence of a large amount of base-stacked structure in a single-stranded PNA in aqueous solvent at room temperature could show some melting transition-like characteristics even though the backbone represents a random coil.

(E) Sequential and Nonsequential Stacking Properties. As the sequential base stacking is constrained by the covalent connection of the backbone, the base-stacking energy can be different for different types of attached backbones. Also the sequential and nonsequential base-stacking interaction may be different because the constraints imposed by the backbone are different for these two cases. Sequential stacking involves only local backbone, while nonsequential stacking involves longer parts of the backbone. Figure 8 represents the time evolution of several sequential (bases G2-T3 and A5-T6 in PNA helix) and nonsequential (bases G4-T8 and A1-T3 in coiled PNA) base-stacking interaction energies. It is found that the average interaction energies are similar in the two cases although the nonsequential stacking energy for the bases G4-T8 in coiled PNA is found to be considerably more favorable during the first half of the dynamic simulation.

(F) Energetics. To describe the helical and coiled conformations of the single strands in terms of interaction energies we have compared the average total self-energy and also the average energy of interaction with the surrounding solvent molecules in the two conformations for each single strand. Table 2 represents the summary of these comparisons. The self-energy is the total intramolecular potential energy of the solute including all interactions (bond, angle, dihedral, improper and electrostatic, and van der Waal) between all atoms in the molecule. It is found

Table 2. Self-Energies and Solvent Interaction Energies of the Different Single Strands in Helical and Coiled States

	PNA		DNA		RNA	
	self	solv	self	solv	self	solv
helix	−365.5 ± 15.0	−448.6±25.2	−248.8±18.6	−1231.3±129.7	−57.7±20.1	−1364.9±66.7
coil	−310.6±15.2	−452.7±24.9	−156.7±18.6	−1373.9±49.9	5.3±17.7	−1439±41.1

Table 3. Components of the Self-Energies of the Backbones of the Three Different Single Strands in Helical and Coiled States

single stand	initial conform	average energy [kcal/mol]				
		bond	angle	torsion	electrostatic	van der Waals
PNA	helix	43 ± 5	107 ± 9	37 ± 3	−230 ± 4	15 ± 5
	coil	43 ± 6	115 ± 9	37 ± 4	−227 ± 4	14 ± 5
DNA	helix	38 ± 5	117 ± 8	57 ± 3	143 ± 16	−4 ± 5
	coil	39 ± 5	110 ± 8	67 ± 3	152 ± 13	−4 ± 5
RNA	helix	47 ± 5	128 ± 7	60 ± 3	316 ± 14	10 ± 6
	coil	46 ± 5	127 ± 8	65 ± 4	270 ± 12	

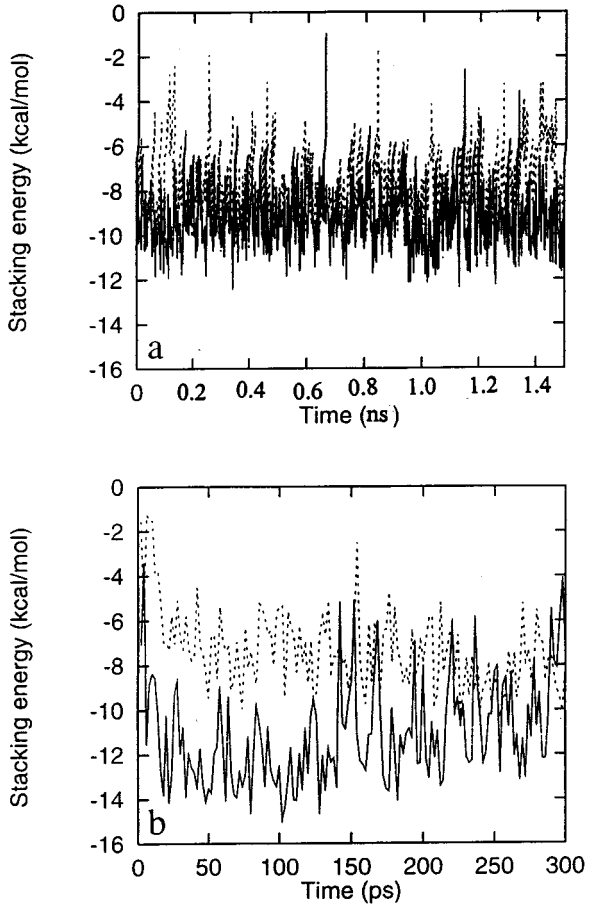

Figure 8. Time evolution of the (a) sequential base stacking between bases G2-T3 (solid line) and the bases A5-T6 (dashed line) in the helical PNA single strand and (b) the nonsequential base stacking between bases G4-T8 (solid line) and A1-T3 (dashed line) in the coiled PNA single strand.

that as far as the self-energy is concerned, the helical conformation is favored considerably over the coiled conformation for each type of single strand. Table 3 compares the different components of the self-energy for only the backbone in the cases of each single strand both in helix and coiled conformations. It is noticeable that the different individual energy terms are very similar or slightly unfavorable for a strand in helix conformation compared to those for a strand in the coiled state. However, the total self-energy (Table 2) shows that the helix conformation is strongly favored over the coiled state in each case. This implies that it is the lack of base stacking which makes the coiled state energetically less favorable compared to helix conformation. It may be pointed out that, in the coil conformations sampled in our work, the average electrostatic energy was very similar to that in the helical conformation of the same strand, indicating that the extended conformation of DNA/RNA backbone in the coil conformation did not gain energetically due to the electrostatic energy minimum.

Examination of the energy of interaction between the single strands and the aqueous solvent (Table 2) indicates that PNA interacts with water rather weakly compared to the interactions of DNA/RNA with water. This is consistent with the fact that the PNA backbone is rather hydrophobic as it contains several CH_2 groups and no polar groups except those involved in peptide groups. On the other hand, the backbones of DNA/RNA being highly hydrophilic interact favorably with surrounding water molecules both in the helical and coiled conformations.

(G) Sugar pucker. Analysis of sugar pucker indicated that for single-stranded DNA and RNA, the sugar in some of the nucleotides adopted both the C2'-endo and C3'-endo pucker conformations for significant time over the entire period of simulations as demonstrated in Figure 9. Such effect is also found for single strands in coiled conformations. The lack of base pairing and base stacking for some bases in single strands may make the corresponding sugar conformation more free and thus allows the sugar to flip more easily and frequently between these two preferred pucker conformations. However, for more convincing results and sequence effects, investigation on several single strands with different mixed sequences would be needed.

(H) Bound Water and Water Bridges. A large number of water molecules were found to hydrogen bond to the single strands (Table 4). The largest number of water molecules were bound to the anionic oxygens of the phosphate groups in the DNA and RNA single strands. Each of these oxygens formed 1.5−2 hydrogen bonds to water, with an average lifetime of 10−20 ps. These oxygens also participated in the largest number of water bridges (eight in the RNA and five in the DNA formed water bridges >50% of the time), in most cases, but not exclusively, with a neighboring phosphate at the other end of the bridge. Only two other groups were found to participate in water bridges >50% of the time: the amino group of A9 in the RNA, and the N7 atom of G4 in the DNA, also with 10-ps lifetimes. In the DNA a smaller number of the O3′, O4′, and O5′ atoms formed hydrogen bonds water, whereas in the ribose of the RNA hydrogen bonds to water were formed by the O2′ atom. Minor groove hydrogen bonding to water involved more atoms in DNA and in PNA than in RNA, with the average hydrogen bond being present 60% of the time in the PNA and 30−40% of the time in the RNA and DNA. In the major groove

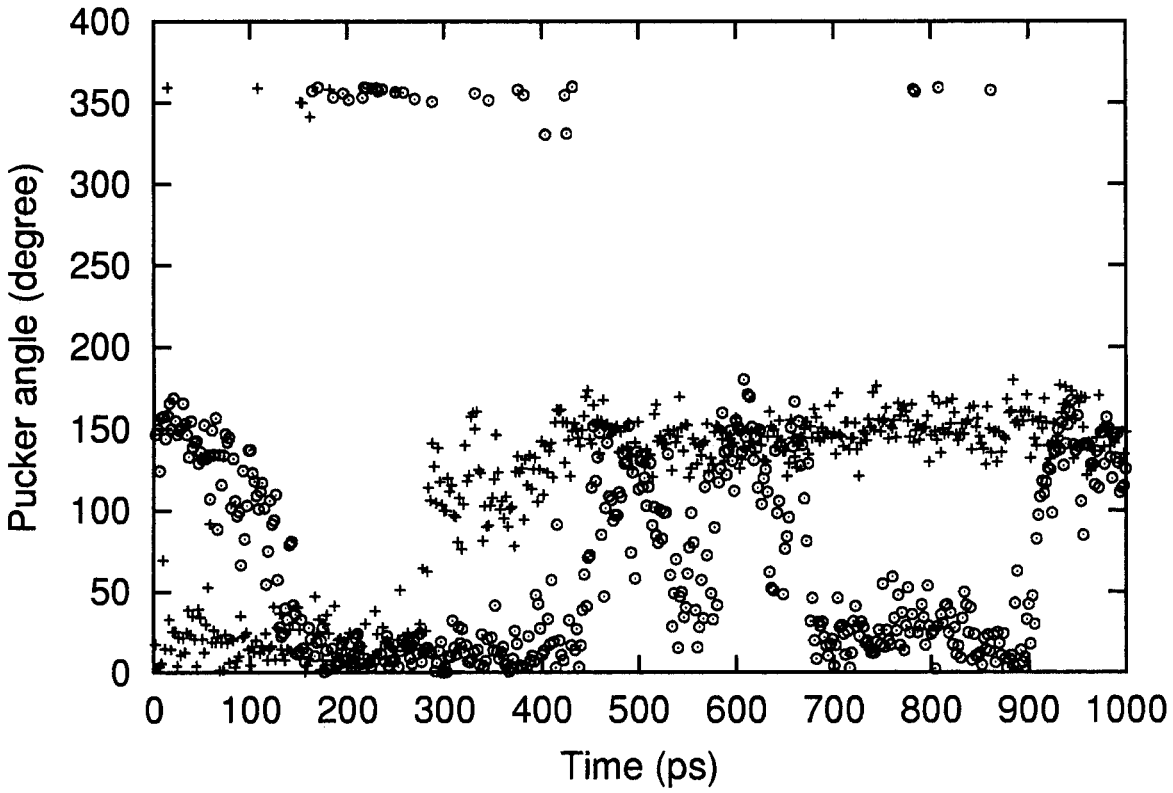

Figure 9. Demonstration of the flipping of the sugar pucker angle for the single-stranded DNA (⊙) and RNA (+) during the dynamics simulations. The data are plotted every 2ps for clarity.

Table 4. Number of Atoms of the Indicated Type That Form Hydrogen Bonds to Water >50% of the Time

atom	PNA	DNA	RNA
phosphate			
O1P, O2P	-	18	18
O3′	-	4	0
O5′	-	2	0
sugar			
O2′	-	-	8
O4′	-	1	0
minor groove			
N3 (A and G)	5	3	0
H21, H22 (G)	1	1	0
O2 (T)	3	3	1
major groove			
O6 (G)	0	0	0
N7 (A and G)	2	2	2
O4 (T)	3	2	1
H61, H62 (A)	0	0	1

the number of atoms involved was approximately equal in all three systems, here too with the hydrogen bonds being formed 30-40% of the time.

The average lifetime of the bound waters was around 10−15 ps, and the longest times for RNA in a single hydrogen bonding event was 244 ps for an RNA anionic phosphate oxygen, while for other atoms it was 90−100 ps in RNA/DNA and 84 ps in PNA. The most long-lived water bridge, 128 ps, was found between a phosphate and an adenine aminogroup in the RNA.

Summary and Conclusions

Analysis of the data obtained from the present investigation by MD simulations of single-stranded PNA, DNA, and RNA in aqueous solvent indicates the following major features.

1. The base−backbone dynamics is less correlated in PNA than in DNA or RNA. This feature appears to be a consequence of the large differences in the covalent structure of base linker parts and also the backbones. In PNA the base is linked to the backbone through a single-bonded chain making the base−backbone coupling weaker than that in the DNA/RNA where the linkage is through a more rigid sugar ring.

2. PNA of the same base sequence maintained its initial base-stacked helix-like regular ordered structure over the entire 1.5-ns dynamic trajectory, while DNA and RNA structures consist of a few locally stacked stretches. The difference in this behavior seems to be partially the consequence of the difference in the strength of coupling between the base and the backbone in the cases of PNA and nucleic acids arising from different covalent structures for PNA and DNA/RNA. PNA is able to maintain its regular sequential stacked arrangement of the bases, allowing considerably more rearrangements in the backbone and the base linker regions than that in DNA/RNA.

3. Comparison of the distribution of the distances between two phosphorus atoms in DNA/RNA or equivalently between two N2′ atoms in PNA and the time evolution of the end-to-end distances in the three different single-stranded helices indicates that RNA is globally more flexible compared to PNA, and DNA has the intermediate position. The local flexibility is very similar for all three different types of single strands. In the cases of DNA and RNA single strands significant flipping of some of the sugar pucker occurred between the C2'-endo and C3'-endo pucker states.

4. In the coiled state both DNA and the RNA single strands adopt structures which are quite extended, while the PNA forms a more compact globular structure which is consistent with the fact that the DNA and the RNA single strands suffer from the intramolecular repulsion between the negatively charged phos-

phate groups, while the PNA consisting of electrically neutral monomeric units is capable of adopting a more compact structure. This property of PNA single strand may cause problems arising from enhanced self-structures and even aggregations with other identical PNA strands in solution.

5. Comparison of the energies of the base stacking in DNA/RNA and PNA indicates that the sequential stacking interaction energies are very similar for the different single strands. Calculation also shows that the "sequential" and the "nonsequential" base stacking are very similar in average interaction strength, although over significant time the nonsequential stacking is found to be considerably stronger than the sequential one.

6. The internal potential energies of all three single-stranded solutes show that the helical conformation is considerably favored over the coiled conformation. Due to the chemical composition PNA is significantly less hydrophilic than the DNA/RNA and thus interacts with water much more weakly than in the case of DNA/RNA. A significant number of water bridges between the base and backbone atoms was found in the cases of the single-stranded DNA and RNA oligomers, while no water bridge was found in PNA involving the base and the backbone.

Acknowledgment. This work was supported by the Swedish Natural Science Research Council.

Supporting Information Available: A representative of the topology file for PNA units (PDF). This material is available free of charge via the Internet at http://pubs.acs.org.

JA0032632